Extended Object Tracking based on Combined Set-Theoretic and Stochastic Fusion

Marcus Baum and **Uwe D. Hanebeck**
Intelligent Sensor-Actuator-Systems Laboratory (ISAS)
Institute for Anthropomatics
Universität Karlsruhe (TH), Germany
mbaum@ira.uka.de, uwe.hanebeck@ieee.org

Abstract – *In this paper, a novel approach for tracking extended objects is presented. The target object is modeled as a circular disc such that the center and extent of the target object can be estimated. At each time step, a finite set of position measurements that are corrupted with stochastic noise may be available. Each position measurement stems from an unknown measurement source on the extended object. In contrast to existing approaches, no statistical assumptions about the distribution of the measurement sources on the extended object are made. As a consequence, it is necessary to deal with stochastic and set-valued uncertainties. For this purpose, a novel combined stochastic and set-theoretic estimator that employs random hyperboloids to express the uncertainties about the true circular disc is derived.*

Keywords: Target Tracking, Extended Objects, Set-Theoretic and Stochastic Estimation, Sensor Data Fusion

1 Introduction

Standard target tracking methods usually consider the tracking of a point source based on noisy measurements. In doing so, it is assumed that the object extension is negligible in comparison to the sensor noise. However, with the increasing resolution of modern sensors, this assumption is often not valid anymore. As a consequence, target tracking algorithms have to take into account that position measurements may stem from different locations on the extended target object. Typically, scenarios for tracking extended objects occur in military surveillance with radar devices [1, 2]. In this context, extended object tracking methods are also used for tracking a collectively moving group of point targets [2]. If the point targets move closely together compared to the sensor resolution, it becomes hard to tackle the data association problem. In this case, it is suitable to consider the group of point targets as one single extended object, since there is a high interdependency between position measurements.

There exists a variety of approaches for incorporating the target extent into target tracking algorithms (for an overview see [1]). For instance, in [3] the motion of the extended object is modeled as one bulk that is characterized by a finite set of individual components (like points on the object) describing physical parameters, e.g., Cartesian displacement. In [4], the target geometry is modeled by means of a spatial distribution. A further recent approach [2] is to model an ellipsoidal object extension with random matrices that are treated as additional state variables.

In this paper, the extended object, which may have an arbitrary shape that is not known, is modeled as a circular disc in the two-dimensional space. At each time step, a finite set of noisy position measurements originating from arbitrary, unknown measurement sources on the extended target may be available. We only require these measurement sources to be on the target surface. In contrast to existing approaches, we do not impose any further (statistical) restrictions or assumptions on the distribution of the measurement sources on the target. This is a major difference to all existing approaches and highly relevant for real world applications. For instance, consider the tracking of a ship with a high-resolution radar device. Due to the (unknown) complex character and shape of the surface of the ship, it is unpredictable which scattering center on the ship is responsible for a particular measurement. It is therefore nearly impossible to determine a reasonable probability distribution for the measurement sources.

The remainder of this paper is structured as follows: After a problem description in Section 2, we first restrict the problem in Section 4 to a static extended object, i.e., a non-moving target with unknown but fixed location and extent. Furthermore, we first consider noise-free measurements (see Section 4.1) such that we can focus on the deterministic part of the problem. It turns out that this deterministic part can be formulated as a set-theoretic estimation problem. In Section 4.2, we incorporate measurements that are corrupted by stochastic noise, which requires a combined set-theoretic and stochastic estimator. Thereupon, Section 5 considers the tracking of an extended object whose position and shape changes with time. Finally, in Section 6 we treat the case that the number of received measurements depends on the size of the extended object. The practicability of the new approach is shown by means of simulations in Section 7.

2 Problem Setup

The problem is to track an extended target object based on noisy position measurements stemming from the target surface. The extended object can have an arbitrary shape that is unknown. In this paper, the true shape of the target object is modeled as the smallest circular disc including the extended object. Hence, from a mathematical point of view, we consider the problem of tracking a *circular disc* with unknown radius and center in the two-dimensional space. A circular disc with center $\left[x^c, y^c\right]^T$ and radius r is denoted with

$$\mathbf{K}(x^c, y^c, r) = \left\{ [x, y]^T \in \mathbb{R}^2 \,|\, (x - x^c)^2 + (y - y^c)^2 \le r^2 \right\}.$$

At each time step k, the parameters of the true circular disc are denoted with a three-dimensional vector $\tilde{\underline{p}}_k = \left[\tilde{x}_k^c, \tilde{y}_k^c, \tilde{r}_k\right]^T$, whose components consist of the center and radius of the smallest circle enclosing the target object.

We consider the problem of estimating $\tilde{\underline{p}}_k$, which is not directly observable. Instead, at each time step k, a finite set of two-dimensional position measurements $\{\hat{\underline{z}}_{k,j}\}_{j=1}^{n_k}$ may be available. Each of these individual measurements $\hat{\underline{z}}_{k,j}$ is the noisy observation of a two-dimensional point $\tilde{\underline{z}}_{k,j}$, named measurement source, which is known to lie in the true circular disc $\mathbf{K}(\tilde{\underline{p}}_k)$, i.e.,

$$\tilde{\underline{z}}_{k,j} \in \mathbf{K}(\tilde{\underline{p}}_k) \text{ and } \hat{\underline{z}}_{k,j} = \tilde{\underline{z}}_{k,j} + \underline{\boldsymbol{w}}_{k,j} \ , \tag{1}$$

where $\underline{\boldsymbol{w}}_{k,j}$ denotes two-dimensional additive white observation noise[1] that models a random Cartesian displacement. The probability distribution of the measurement noise $\underline{\boldsymbol{w}}_{k,j}$ is assumed to be known. On the other hand, the measurement source $\tilde{\underline{z}}_{k,j}$ is totally unknown such that we do not know which point on the extended object was actually measured by $\hat{\underline{z}}_{k,j}$. Hence, the measurement model suffers from a set-valued uncertainty *and* a stochastic uncertainty. Note that neither the measurement source $\tilde{\underline{z}}_{k,j}$ on the extended object nor the number of measurements n_k at time step k are assumed to be drawn from a particular probability distribution. Nonetheless, later we will also consider the case that the number of measurements n_k depends on the size of the extended object.

The position as well as the shape of the extended object may vary over time. The temporal evolution of the (smallest) circular disc, which includes the extended object, is modeled by means of a so-called *extended motion model* that captures both the motion and the extent of the target object (details are given Section 5).

3 Getting Intuition: Known Extent

In order to obtain some insights on combined set-theoretic and statistical estimation of extended objects, we first consider the special case of estimating the unknown but fixed location of a target object with known, fixed extent. For the sake of an intuitive explanation, we omit the detailed formulas in this section. Details can be found in Remark 6 as a special case of the general problem.

If the extent of the target object is known, the true radius $\tilde{r}$ of the smallest enclosing circle of the target is also known and the unknown center $\left[\tilde{x}^c, \tilde{y}^c\right]^T$ is desired. We first only consider noise-free measurements $\hat{\underline{z}}_k$ such that $\hat{\underline{z}}_k \in \mathbf{K}(\left[\tilde{x}^c, \tilde{y}^c, \tilde{r}\right]^T)$ holds, which is equivalent to $\left[\tilde{x}^c, \tilde{y}^c\right]^T \in \mathbf{K}(\left[\hat{\underline{z}}_k^T, \tilde{r}\right]^T)$. Hence, all possible centers $\left[\tilde{x}^c, \tilde{y}^c\right]^T$ that are consistent with $\hat{\underline{z}}_k$ are an element of a circular disc with center $\hat{\underline{z}}_k$ and radius $\tilde{r}$. This set is called *measurement solution set*. At a fixed time step k, the accumulated knowledge about the true center is given by the intersection of all measurement solution sets that are available so far. This set is called *solution set*. Unfortunately, the exact solution set is in general not a basic geometric shape such that recursive computation is intractable. It is therefore common in set-theoretic estimators [5] to bound the exact solution set conservatively with a basic geometric shape. In this particular case, it is suitable to represent the solution set as a circular disc again. In doing so, whenever a new measurement is received, the intersection between the corresponding measurement solution set and the current solution set has to be bounded conservatively with the smallest possible circular disc. With an increasing number of measurements, the radius of the solution set shrinks and the center of the solution set approaches the true center.

If $\hat{\underline{z}}_k$ is a noisy measurement of $\tilde{\underline{z}}_k$ according to $\hat{\underline{z}}_k = \tilde{\underline{z}}_k + \underline{\boldsymbol{w}}_k$, the knowledge about $\tilde{\underline{z}}_k$ is given by the random variable $\hat{\underline{z}}_k - \underline{\boldsymbol{w}}_k$. As a consequence, a measurement $\hat{\underline{z}}_k$ yields a random measurement solution set, namely a circular disc, with random center $\hat{\underline{z}}_k - \underline{\boldsymbol{w}}_k$ but fixed radius $\tilde{r}$. The solution sets then become random circular discs, whose center and radius are random. At each time step, the random measurement solution set has to be intersected with the current random solution set (conditioned on non-emptiness). Thus, a combined set-theoretic and stochastic estimator [6, 7] is obtained. With an increasing number of measurements, the set-valued and stochastic uncertainties vanish.

4 Static Extended Object

4.1 Noise-free Measurements

In case of estimating both the location and extent of a static extended object for given measurements not corrupted by noise, we assume w.l.o.g. that at each time step k one position measurement $\hat{\underline{z}}_k = \tilde{\underline{z}}_k \in \mathbb{R}^2$ is given. Each $\hat{\underline{z}}_k$ represents a point that is known to lie in the true smallest enclosing circle of the target object $\mathbf{K}(\tilde{p})$, i.e., $\hat{\underline{z}}_k \in \mathbf{K}(\tilde{p})$.

In the following, we derive a set-theoretic estimator [5] for the parameters $\tilde{p} \in \Omega := \mathbb{R}^2 \times \mathbb{R}^+$ of the true circular disc $\mathbf{K}(\tilde{p})$ based on the measurements $\hat{\underline{z}}_k$. Consider a particular measurement $\hat{\underline{z}}_k = \left[x_k^m, y_k^m\right]^T$ at time step k. We know that the true circular disc $\mathbf{K}(\left[\tilde{x}^c, \tilde{y}^c, \tilde{r}\right]^T)$ includes $\hat{\underline{z}}_k$, i.e., $\hat{\underline{z}}_k \in \mathbf{K}(\left[\tilde{x}^c, \tilde{y}^c, \tilde{r}\right]^T)$. Hence, for a given measurement $\hat{\underline{z}}_k$, we can conclude that $\left[\tilde{x}^c, \tilde{y}^c, \tilde{r}\right]^T$ is an element of the set of

---

[1]Note that all random variables are printed bold face in this paper.

all feasible parameter vectors

$$\left\{ \left[x^c, y^c, r\right]^T \in \Omega \mid (x_k^m - x^c)^2 + (y_k^m - y^c)^2 \leq r^2 \right\}. \quad (2)$$

This set is also called measurement solution set and denoted by Δ_k^m. In fact, Δ_k^m is a cone oriented along the r–axis with apex $\left[x_k^m, y_k^m, 0\right]^T$ and perpendicular cone angle.

The solution set Δ_k^e for the true parameter vector $\tilde{p}$ given the measurements $\hat{\underline{z}}_1, \ldots, \hat{\underline{z}}_k$ can be computed recursively according to

$$\Delta_k^e = \Delta_{k-1}^e \cap \Delta_k^m \quad (3)$$

with $\Delta_1^e := \Delta_1^m$.

Example 1. In Figure 1a, an extended object with a rectangular shape is shown. Furthermore, the first two measurements $\hat{\underline{z}}_1$ and $\hat{\underline{z}}_2$ are depicted by red markers. The bounds of the corresponding cones Δ_1^m and Δ_2^m in the parameter-space are shown in Figure 1b. The entire sets Δ_1^m and Δ_2^m are given by all points that lie "above" the plotted bounds. Since $\hat{\underline{z}}_1$ and $\hat{\underline{z}}_2$ both lie in the true circular disc, the true parameters are elements of $\Delta_2^e = \Delta_1^m \cap \Delta_2^m$. Figure 1c and 1d illustrate an example of the solution set Δ_4^e for four received measurements. The red markers in Figure 1c indicate the positions of the received measurements in the two-dimensional state-space. The discs $\mathbf{K}(\tilde{\underline{p}}_4), \mathbf{K}(\underline{p}_4^1)$ and $\mathbf{K}(\underline{p}_4^2)$ are examples for feasible circular discs. $\mathbf{K}(\underline{p}_4^1)$ represents the smallest enclosing circle of the given measurements. In this example, $\mathbf{K}(\tilde{\underline{p}}_4)$ is the true disc, since it is the smallest disc which includes the rectangular extended object. In Figure 1d, the bound of the set Δ_4^e and the parameters of the example discs are depicted. Note that Δ_4^e is neither a cone nor any other basic geometric object.

The result of an estimation procedure is typically a point estimate, i.e., a single value, rather than a set. Justified by the following Remark 1, the apex[2] of Δ_k^e can serve as a proper point estimate for $\tilde{p}$.

Remark 1. If the measurements cover the entire area of the target in the course of time, with an increasing number of measurements, the apex of Δ_k^e (the unique point in Δ_k^e with the smallest r–coordinate) converges to the parameter vector $\tilde{p}$ of the smallest enclosing circle $\mathbf{K}(\tilde{p})$ of the target object.

The exact recursive computation of Δ_k^e is computationally intractable since there is in general no proper parametric description of the set Δ_k^e. Note that the intersection of two cones in the form of Equation (2) is not a cone again. In order to tackle this problem, we make use of the fact, that the intersection of a cone and a hyperboloid (see Definition 1) can be approximated conservatively by a hyperboloid. This novel approximation allows recursively bounding Δ_k^e with hyperboloids such that the convergence property stated in Remark 1 is preserved.

Definition 1 (Hyperboloid of Revolution)**.** The upper sheet of a two-sheeted circular hyperboloid of revolution is given by
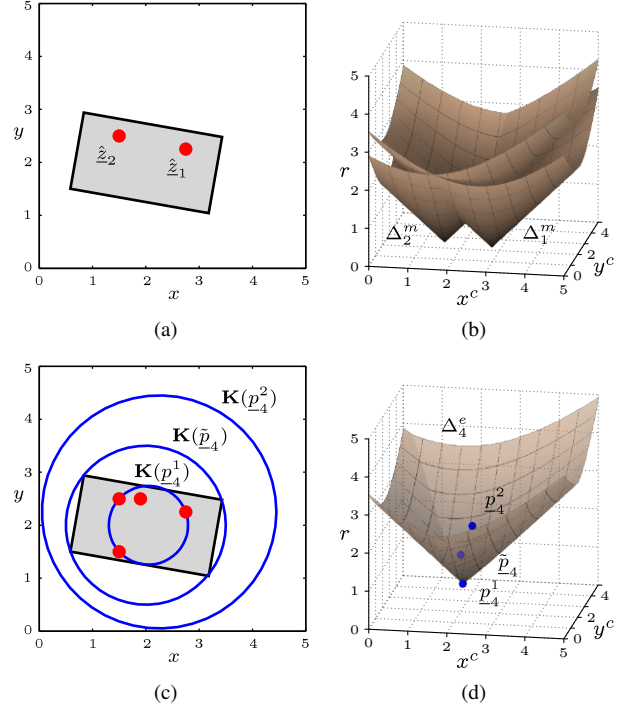

Figure 1: Set-theoretic estimation of an extended object.

$$\mathbf{H}(x^e, y^e, z^e, a) := \left\{ \left[x^c, y^c, r\right]^T \in \mathbb{R}^3 \mid r \geq z^e \text{ and} \right.$$
$$\left. (x^c - x^e)^2 + (y^c - y^e)^2 + a^2 \leq (r - z^e)^2 \right\}$$

with $x^e, y^e, z^e \in \mathbb{R}$ and $a \in \mathbb{R}^+$.

Remark 2. A hyperboloid $\mathbf{H}(x^e, y^e, z^e, a)$ has the following properties (see Figure 2a):

- the focus is $F = \left[x^e, y^e, z^e\right]^T$,
- the apex is located at $A = \left[x^e, y^e, a + z^e\right]^T$,
- the cone angle is orthogonal, and
- the hyperboloid is oriented along the r–axis.

Definition 2. A hyperboloid of the form $\mathbf{H}(x^e, y^e, 0, a)$ is abbreviated with $\underline{\mathbf{H}}(x^e, y^e, a)$. Furthermore, the set $\underline{\mathbf{C}}(x^e, y^e) := \mathbf{H}(x^e, y^e, 0, 0)$ is a cone oriented along the r–axis whose apex lies on the $x^c y^c$–plane.

A set-theoretic estimator for the parameters $\tilde{\underline{p}}_k$ of the true circular disc can be constructed in the following way:

Set-Theoretic Estimator (STE) 1
- **Solution Set**
  The solution set is given by a hyperboloid $\underline{\mathbf{H}}(\underline{p}_k^e)$ with $\underline{p}_k^e = \left[x_k^e, y_k^e, a_k^e\right]^T$. $\underline{\mathbf{H}}(\underline{p}_k^e)$ is a conservative approximation of the exact solution set Δ_k^e, i.e., $\Delta_k^e \subset \underline{\mathbf{H}}(\underline{p}_k^e)$.
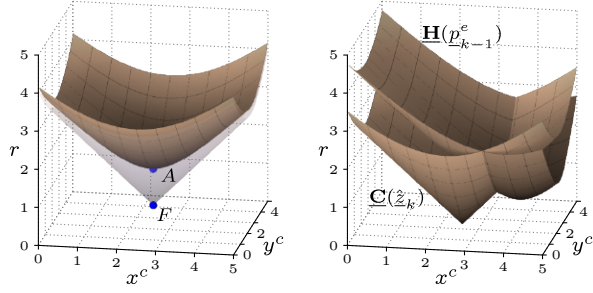- **Measurement Solution Set**
  A measurement $\hat{\underline{z}}_k$ yields a measurement solution set $\underline{\mathbf{C}}(\hat{\underline{z}}_k)$ (see Equation (2)), i.e., $\Delta_k^m = \underline{\mathbf{C}}(\hat{\underline{z}}_k)$.
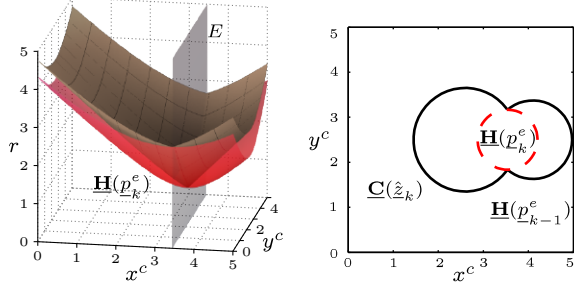- **Fusion**
  Fusing $\underline{\mathbf{H}}(\underline{p}_{k-1}^e)$ with $\underline{\mathbf{C}}(\hat{\underline{z}}_k)$ results in $\underline{\mathbf{H}}(\underline{p}_k^e)$, whereas

$$\underline{\mathbf{H}}(\underline{p}_{k-1}^e) \cap \underline{\mathbf{C}}(\hat{\underline{z}}_k) \subset \underline{\mathbf{H}}(\underline{p}_k^e) \ .$$

(a) A hyperboloid with apex A and focus F.

(b) A cone $\underline{\mathbf{C}}([2.5, 2]^T)$ and a hyperboloid $\underline{\mathbf{H}}([4, 2, 1]^T)$.

(c) Approximated intersection.

(d) $x^c y^c$–plane for fixed $r = 1.8$.

Figure 2: Approximating the intersection of a cone and a hyperboloid with a hyperboloid.

The function, which maps $\underline{p}^e_{k-1}$ and $\hat{\underline{z}}_k$ to $\underline{p}^e_k$, is denoted with $\mathcal{G}_1(\cdot)$ so that

$$\underline{p}^e_k = \mathcal{G}_1(\hat{\underline{z}}_k, \underline{p}^e_{k-1}) \text{ with } \underline{p}^e_1 = \begin{bmatrix} \hat{\underline{z}}_1 \\ 0 \end{bmatrix} . \quad (4)$$

- **Point Estimate**
  The point estimate for $\tilde{p}$ at time step k is given by the apex $\underline{p}^e_k$ of $\underline{\mathbf{H}}(\underline{p}^e_k)$.

A proper function $\mathcal{G}_1(\cdot)$ can be constructed on the basis of the following Theorem 1, which is based on the observation that the intersection of the bounds[3] $\partial\underline{\mathbf{H}}(\underline{p}^e_{k-1})$ and $\partial\underline{\mathbf{C}}(\hat{\underline{z}}_k)$ is a hyperbola lying in a plane perpendicular to the $x^c y^c$–plane (see Figure 2).

Theorem 1. *Given are a cone $\underline{\mathbf{C}}(\hat{\underline{z}}_k)$ and a hyperboloid $\underline{\mathbf{H}}(\underline{p}^e_{k-1})$. Furthermore, let*

$$d := \sqrt{(\hat{x}^m_k - x^e_{k-1})^2 + (\hat{y}^m_k - y^e_{k-1})^2}$$

denote the distance between the vectors $[\hat{x}^m_k, \hat{y}^m_k]^T$ and $[x^e_{k-1}, y^e_{k-1}]^T$. If the following condition

$$d > a^e_{k-1} \quad (5)$$

holds, the hyperboloid $\underline{\mathbf{H}}(\underline{p}^e_k)$ with

$$\begin{bmatrix} x^e_k \\ y^e_k \end{bmatrix} = \begin{bmatrix} \hat{x}^m_k \\ \hat{y}^m_k \end{bmatrix} + a^e_k \cdot \frac{1}{d}(\begin{bmatrix} x^e_{k-1} \\ y^e_{k-1} \end{bmatrix} - \begin{bmatrix} \hat{x}^m_k \\ \hat{y}^m_k \end{bmatrix}) \quad (6)$$

$$a^e_k = \frac{1}{2}(d + \frac{(a^e_{k-1})^2}{d}) \quad (7)$$

---

[3]The operator ∂ denotes the bound of a set.

has the following properties:

1. *The apex of $\underline{\mathbf{C}}(\hat{\underline{z}}_k) \cap \underline{\mathbf{H}}(\underline{p}^e_{k-1})$ (i.e., the unique point with the smallest r–coordinate in $\underline{\mathbf{C}}(\hat{\underline{z}}_k) \cap \underline{\mathbf{H}}(\underline{p}^e_{k-1})$) coincides with the apex $\underline{p}^e_k$ of $\underline{\mathbf{H}}(\underline{p}^e_k)$.*

2. *The intersection of $\partial\underline{\mathbf{C}}(\hat{\underline{z}}_k) \cap \partial\underline{\mathbf{H}}(\underline{p}^e_{k-1})$ is a hyperbola that lies in a plane E with normal vector $[x^e_{k-1} - \hat{x}^m_k, y^e_{k-1} - \hat{y}^m_k, 0]^T$ and position vector $\underline{p}^e_k$.*

3. $E \cap \partial\underline{\mathbf{H}}(\underline{p}^e_k) = \partial\underline{\mathbf{C}}(\hat{\underline{z}}_k) \cap \partial\underline{\mathbf{H}}(\underline{p}^e_{k-1})$

4. $\underline{\mathbf{C}}(\hat{\underline{z}}_k) \cap \underline{\mathbf{H}}(\underline{p}^e_{k-1}) \subseteq \underline{\mathbf{H}}(\underline{p}^e_k)$

Proof. Can be shown with basic algebraic rules. □

Remark 3. Condition (5) states that the projection of the apex of $\underline{\mathbf{C}}(\hat{\underline{z}}_k) \cap \underline{\mathbf{H}}(\underline{p}^e_{k-1})$ onto the $x^c y^c$–plane lies on the segment from $[\hat{x}^m_k, \hat{y}^m_k, 0]^T$ to $[x^e_{k-1}, y^e_{k-1}, 0]^T$. An equivalent condition is the requirement that the r–coordinate of the apex of $\underline{\mathbf{C}}(\hat{\underline{z}}_k) \cap \underline{\mathbf{H}}(\underline{p}^e_{k-1})$ is greater than a^e_{k-1}.

Definition 3. The function $\mathcal{G}_1 : \mathbb{R}^2 \times \mathbb{R}^3 \to \mathbb{R}^3$ in Equation (4) is defined as

$$\mathcal{G}_1(\hat{\underline{z}}_k, \underline{p}^e_{k-1}) = \begin{cases} \mathcal{G}^*_1(\hat{\underline{z}}_k, \underline{p}^e_{k-1}) & \text{if Condition (5) holds} \\ \underline{p}^e_{k-1} & \text{otherwise} \end{cases}$$

in which $\mathcal{G}^*_1 : \mathbb{R}^2 \times \mathbb{R}^3 \to \mathbb{R}^3$ denotes the total function defined by Equation (6) and (7) that maps $\hat{\underline{z}}_k$ and $\underline{p}^e_{k-1}$ to $\underline{p}^e_k$.

Remark 4. Condition (5) holds if and only if the disc with the minimal radius in the current solution set (which is given by the apex) does *not* include the received measurement. If Condition (5) holds, the incorporation of the measurement increases the r–coordinate of the apex of the current solution set and thus increases the minimal possible radius. On the other hand, if Condition (5) does not hold, the disc with the minimal radius in the solution set already includes the received measurement.

From Remark 4 it follows, that the apex of $\underline{\mathbf{H}}(\underline{p}^e_k)$, namely $\underline{p}^e_k$, converges to the parameters of the true disc $\tilde{\mathbf{K}}(\tilde{p})$ if for each time step k, the future measurements $\hat{\underline{z}}_l$ with $l \geq k$ cover the entire extended object. Hence, the approximation performed with $\mathcal{G}_1(\cdot)$ preserves the convergence property stated in Remark 1 and is thus valid. Furthermore, this property justifies to choose $\underline{p}^e_k$ from $\underline{\mathbf{H}}(\underline{p}^e_k)$ as a point estimate.

Example 2. Figure 3b depicts an example of the resulting hyperboloid $\underline{\mathbf{H}}(\underline{p}^e_4)$ in the parameter-space after four measurements. The disc $\mathbf{K}(\underline{p}^e_4)$ (see Figure 3a), does not include all received measurements, because $\underline{\mathbf{H}}(\underline{p}^e_4)$ is a conservative approximation of the true solution set Δ^e_4, i.e., $\underline{p}^e_4 \in \underline{\mathbf{H}}(\underline{p}^e_4)$ but $\underline{p}_4 \notin \Delta^e_4$. Nonetheless, $\tilde{p}$ is an element of $\underline{\mathbf{H}}(\underline{p}^e_4)$.

Remark 5. A related problem is the minimal enclosing circle problem [8]. These algorithms are not feasible for the problem under consideration, since they are not suitable to be computed recursively with random points and do not supply all feasible circles.
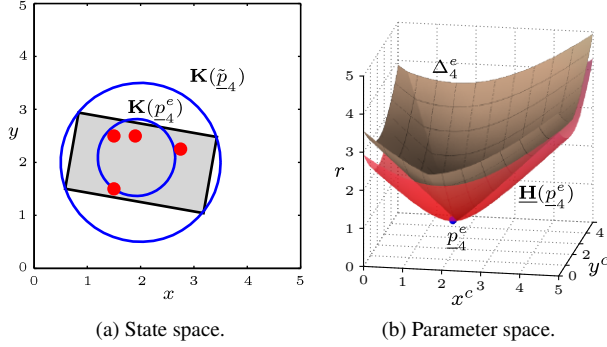
(a) State space.   (b) Parameter space.

Figure 3: Outer-bounding the true solution set.

(a) State space with noisy measure-(b) 90%–covariance ellipsoid and
ments and estimated disc.   mean $\hat{\underline{p}}_4^e$ (blue dot) of $\underline{p}_4^e$.

Figure 4: Estimation of a static circular disc given noisy measurements.

4.2   Noisy Measurements

The next step is to consider the problem of estimating a static extended object from measurements corrupted by stochastic noise. W.l.o.g. we assume that at each time step one (noisy) position measurement $\hat{\underline{z}}_k$ is available. The measurement $\hat{\underline{z}}_k$ is a noisy observation of the measurement source $\tilde{\underline{z}}_k$ according to (see Section 2): $\tilde{\underline{z}}_k \in \mathbf{K}(\tilde{\underline{p}}_k)$ and $\hat{\underline{z}}_k = \tilde{\underline{z}}_k + \underline{w}_k$. The term $\underline{w}_k$ denotes white measurement noise. Since the measurement source is unknown, no prior information about $\tilde{\underline{z}}_k$ is available. Thus, the knowledge about $\tilde{\underline{z}}_k$ is given by the random vector $\hat{\underline{z}}_k - \underline{w}_k$ and we obtain the condition $\hat{\underline{z}}_k - \underline{w}_k \in \mathbf{K}(\tilde{\underline{p}}_k)$, which holds if and only if $\tilde{\underline{p}}_k \in \underline{\mathbf{C}}(\hat{\underline{z}}_k - \underline{w}_k)$. As a consequence, the measurement solution sets become random cones $\boldsymbol{\Delta}_k^m = \underline{\mathbf{C}}(\hat{\underline{z}}_k - \underline{w}_k)$. In analogy to Equation (3), a recursive update scheme is given by $\boldsymbol{\Delta}_k^e = \boldsymbol{\Delta}_{k-1}^e \cap \boldsymbol{\Delta}_k^m$ but now $\boldsymbol{\Delta}_k^e$ and $\boldsymbol{\Delta}_k^m$ are random sets. As in Section 4, there is no parametric description of $\boldsymbol{\Delta}_k^e$ such that we have to perform a conservative approximation with hyperboloids again. In this manner, a combined set-theoretic and stochastic estimator that uses random sets to capture the set-valued *and* stochastic uncertainty can be constructed.

Stochastic and Set-Theoretic Estimator (SSTE) 1
- **Random Solution Set**
  The uncertainty about the current state is expressed with a random hyperboloid $\mathbf{H}(\underline{p}_k^e)$, where $\underline{p}_k^e = \left[\boldsymbol{x}_k^e, \boldsymbol{y}_k^e, \boldsymbol{a}_k^e\right]^T$ is a random vector. In the following, we assume that $\underline{p}_k^e \sim \mathcal{N}(p; \hat{\underline{p}}_k^e, \mathbf{C}_k^e)$.
- **Random Measurement Solution Set**
  $\hat{\underline{z}}_k$ yields an uncertain cone $\underline{\mathbf{C}}(\underline{z}_k)$ with $\underline{z}_k := \hat{\underline{z}}_k - \underline{w}_k$. We assume that $\underline{z}_k \sim \mathcal{N}(z; \hat{\underline{z}}_k, \mathbf{C}_k^z)$.
- **Fusion**
  $\mathbf{H}(\underline{p}_k^e)$ is the result of approximating the intersection $\mathbf{H}(\underline{p}_{k-1}^e)$ and $\underline{\mathbf{C}}(\underline{z}_k)$ according to
  $$\underline{p}_k^e = \mathcal{G}_1(\underline{z}_k, \underline{p}_{k-1}^e) \text{ and } \underline{p}_1^e = \begin{bmatrix} \underline{z}_1 \\ 0 \end{bmatrix} \quad . \qquad (8)$$
- **Point Estimate**
  A proper point estimate at time step k is given by $\hat{\underline{p}}_k^e$ with covariance matrix $\mathbf{C}_k^e$.
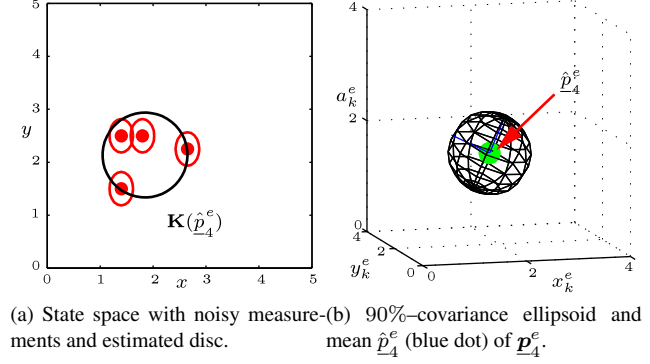
In contrast to the deterministic case, the function $\mathcal{G}_1(\cdot)$ in Equation (8) has to be evaluated stochastically, i.e., the arguments are random variables. In general, the distribution of $\underline{p}_k^e$ cannot be computed in closed form for given distributions of $\underline{z}_k$ and $\underline{p}_{k-1}^e$, since $\mathcal{G}_1(\cdot)$ is a nonlinear function. Nevertheless, the distribution of $\underline{p}_k^e$ can be approximated with a Gaussian distribution by employing the prediction step of a nonlinear stochastic state estimator. Therefore, it is useful to rewrite Equation (8) as $\underline{p}_k^e = \mathcal{G}_1(\underline{b}_k)$ with $\underline{b}_k = \left[(\underline{z}_k)^T, (\underline{p}_{k-1}^e)^T\right]^T$. The mean and covariance matrix of $\underline{b}_k$ are given by $\left[(\hat{\underline{z}}_k)^T, (\hat{\underline{p}}_{k-1}^e)^T\right]^T$ and $\mathrm{diag}(\mathbf{C}_k^z, \mathbf{C}_{k-1}^e)$. Note that due to the assumption of white measurement noise, the cross covariance matrices of $\underline{z}_k$ and $\underline{p}_{k-1}^e$ are zero matrices. Since $\mathcal{G}_1(\cdot)$ is not differentiable due to a case distinction in its definition, linearization is not possible such that state estimators based on deterministic sampling like the Gaussian Filter [9] and the UKF [10] are suitable.

Example 3 (UKF)**.** Figure 4 illustrates the result of SSTE 1 after receiving four measurements with measurement noise $\mathbf{C}_k^z = \mathrm{diag}(0.2, 0.4)$. The unscented transformation [10] was used to evaluate Equation (8). Figure 4a shows the state-space with the measurements, the σ–covariance ellipses of $\mathbf{C}_k^z$ and the point estimate $\mathbf{K}(\hat{\underline{p}}_4^e)$ (black). Figure 4b depicts the three-dimensional parameter-space (for hyperboloids) with the mean and 90%–covariance ellipsoid of $\underline{p}_4^e$.

Remark 6. If the true radius $\tilde{r}$ is known, the probability density function $f(\underline{p}_k^e)$ of $\underline{p}_k^e$ in SSTE 1 can be updated (at each time step) with the true radius by computing the posterior pdf $f(\underline{p}_k^e | \{\boldsymbol{a}_k^e \leq \tilde{r}\})$ what corresponds to truncating infeasible values. Note that for $\boldsymbol{a}_k^e > \tilde{r}$ there is no disc with radius $\tilde{r}$ in $\underline{\mathbf{H}}(\underline{p}_k^e)$. In this way, the estimator described intuitively in Section 3 is obtained. The two-dimensional random solution set for the desired center is $\mathbf{K}(\boldsymbol{x}_k^e, \boldsymbol{y}_k^e, \sqrt{(\tilde{r})^2 - (\boldsymbol{a}_k^e)^2})$ given that $\boldsymbol{a}_k^e \leq \tilde{r}$. In this context, see also Figure 2d.

If the support of the measurement noise $\underline{w}_k$ is bounded, SSTE 1 converges to the true circular disc plus the bounded support. Otherwise, in general SSTE 1 does not converge

to a fixed point. This is a direct consequence of the measurement model (1), which does not allow to tell set-valued and stochastic uncertainties apart. There are two possibilities to cope with this behavior. First, one can assume the noise to be bounded and subtract the (known) support afterwards from the estimated circular disc. This subtraction can be performed in a purely geometric fashion. In doing so, SSTE 1 converges to the true circular disc. The second solution, which is employed in Section 6, is to incorporate further knowledge that allows to separate set-valued and stochastic uncertainties.

5 Dynamic Extended Object

In order to track an extended object that moves and varies its shape over time, random solution sets have to be propagated through an (extended) motion model. To capture translations along the r–axis (which models the scaling of the true disc), it becomes necessary to represent solution sets with hyperboloids of the form $\mathbf{H}([x_k^e, y_k^e, z_k^e, a_k^e]^T)$ instead of $\underline{\mathbf{H}}([x_k^e, y_k^e, a_k^e]^T)$. The suggested estimator for tracking an extended object SSTE 2 is sketched in the following. A more detailed description of the particular components is given subsequently.

Stochastic and Set-Theoretic Estimator (SSTE) 2

- **Random Solution Set**
  The random solution set is represented with a random hyperboloid $\mathbf{H}(\underline{p}_k^e)$, where $\underline{p}_k^e \sim \mathcal{N}(\underline{p}; \hat{\underline{p}}_k^e, \mathbf{C}_k^e)$. Note that throughout the rest of this paper, the parameter vector $\underline{p}_k^e$ is of the form $[x_k^e, y_k^e, z_k^e, a_k^e]^T$.
- **Random Measurement Solution Set**
  The measurements $\{\hat{\underline{z}}_{k,j}\}_{j=1}^{n_k}$ at time step k lead to random cones $\underline{\mathbf{C}}(\underline{z}_{k,0}), \ldots, \underline{\mathbf{C}}(\underline{z}_{k,n_k})$ where $\underline{z}_{k,j} := \hat{\underline{z}}_{k,j} - \underline{w}_{k,j}$.
- **Prediction**
  The predicted random solution set $\mathbf{H}(\underline{p}_k^p)$ results from propagating $\mathbf{H}(\underline{p}_{k-1}^e)$ through the extended motion model given by Equation (9).
- **Fusion**
  $\mathbf{H}(\underline{p}_k^e)$ is the result of bounding $\bigcap_j \underline{\mathbf{C}}(\underline{z}_{k,j}) \cap \mathbf{H}(\underline{p}_k^p)$ conservatively. Furthermore, $\underline{p}_1^e = [\underline{z}_1^T, 0, 0]^T$.
- **Point Estimate**
  A proper point estimate of $\tilde{\underline{p}}_k$ is given by the expected apex of $\mathbf{H}(\underline{p}_k^e)$. With $\mathbf{B}_2 := \begin{bmatrix} 1 & 0 & 0 & 0 \\ 0 & 1 & 0 & 0 \\ 0 & 0 & 1 & 1 \end{bmatrix}$, the point estimate is given by $\mathbf{B}_2\hat{\underline{p}}_k^e$ with covariance matrix $\mathbf{B}_2\mathbf{C}_k^p\mathbf{B}_2^T$.

In order to propagate a random solution set to the next time step, it must be ensured that the propagated set is again a hyperboloid. In this paper, we therefore only consider linear *extended motion models* of the form

$$\underline{p}_k = \mathbf{A}_k\underline{p}_{k-1} + \mathbf{B}_k(\hat{\underline{u}}_{k-1} + \underline{v}_{k-1}) \ , \qquad (9)$$
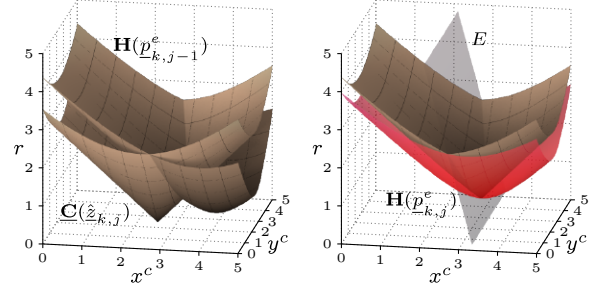
(a) A cone $\underline{\mathbf{C}}([2.5, 2]^T)$ and a hyperboloid $\mathbf{H}([4, 2, -0.5, 1]^T)$.

(b) Approximated intersection.

Figure 5: Approximating the intersection of a cone and a hyperboloid (brown) with a hyperboloid (red).

which map the parameters $\underline{p}_{k-1}$ of the circular disc at time step $k-1$ to the parameters $\underline{p}_k$ at time step k. The zero-mean Gaussian distributed random vector $\underline{v}_{k-1}$ models input noise and $\hat{\underline{u}}_{k-1}$ denotes the deterministic system input. Furthermore, we assume that $\mathbf{A}_k = \text{diag}(\mathbf{A}_k^*, 1)$ where $\mathbf{A}_k^*$ is a two-dimensional rotation matrix. Note that Equation (9) defines a congruent mapping from $\underline{p}_{k-1}$ to $\underline{p}_k$ for given $\underline{v}_{k-1}$. Consider the random solution set $\mathbf{H}(\underline{p}_{k-1}^e)$ at time step $k-1$. Each point in $\mathbf{H}(\underline{p}_{k-1}^e)$ specifies a feasible circular disc that has to be propagated through the extended motion model given by Equation (9). Due to the special form of Equation (9), the set $\mathbf{A}_k\mathbf{H}(\underline{p}_{k-1}^e) + \mathbf{B}_k(\hat{\underline{u}}_{k-1} + \underline{v}_{k-1})$ is again a hyperboloid $\mathbf{H}(\underline{p}_k^p)$ with parameter vector

$$\underline{p}_k^p = \begin{bmatrix} \mathbf{A}_k & 0 \\ 0 & 1 \end{bmatrix} \underline{p}_{k-1}^e + \begin{bmatrix} \mathbf{B}_k \\ 0 \end{bmatrix} (\hat{\underline{u}}_{k-1} + \underline{v}_{k-1}) \ . \qquad (10)$$

Since Equation (10) is linear, $\underline{p}_k^p$ is Gaussian distributed, in case $\underline{p}_{k-1}^e$ is Gaussian distributed and $\underline{v}_{k-1}$ is Gaussian noise. The mean and covariance matrix of $\underline{p}_k^p$ can be computed with the well-known Kalman filter prediction step:

$$\hat{\underline{p}}_k^p = \begin{bmatrix} \mathbf{A}_k & 0 \\ 0 & 1 \end{bmatrix} \hat{\underline{p}}_{k-1}^e + \begin{bmatrix} \mathbf{B}_k \\ 0 \end{bmatrix} \hat{\underline{u}}_{k-1}, \text{and} \qquad (11)$$

$$\mathbf{C}_k^p = \begin{bmatrix} \mathbf{A}_k & 0 \\ 0 & 1 \end{bmatrix} \mathbf{C}_{k-1}^e \begin{bmatrix} \mathbf{A}_k & 0 \\ 0 & 1 \end{bmatrix}^T + \begin{bmatrix} \mathbf{C}_{k-1}^v & 0 \\ 0 & 0 \end{bmatrix} \ . \qquad (12)$$

The fusion step of SSTE 2 consists of approximating the intersection of $\mathbf{H}(\underline{p}_k^p)$ and the cones $\underline{\mathbf{C}}(\hat{\underline{z}}_{k,j})$ conservatively with a hyperboloid $\mathbf{H}(\underline{p}_k^e)$. This intersection can be performed recursively by setting $\underline{p}_{k,0}^e := \underline{p}_k^p$ and computing the hyperboloid $\mathbf{H}(\underline{p}_{k,j}^e)$ that bounds $\mathbf{H}(\underline{p}_{k,j-1}^e) \cap \underline{\mathbf{C}}(\hat{\underline{z}}_{k,j})$ (for $1 \le j \le n_k$). The parameters of the random solution set at time step k are then given by $\underline{p}_k^e := \underline{p}_{k,n_k}^e$. A proper function $\mathcal{G}_2(\cdot)$ that maps $\hat{\underline{z}}_{k,j}$ and $\underline{p}_{k,j-1}^e$ to $\underline{p}_{k,j}^e$ can be constructed by means of Theorem 2 which is actually an extension of Theorem 1 to hyperboloids that may be translated along the r–axis. Theorem 2 is based on the observation that the intersection of $\partial\underline{\mathbf{C}}(\hat{\underline{z}}_{k,j})$ and $\partial\mathbf{H}(\underline{p}_{k,j-1}^e)$ is a hyperbola lying in a plane (see Figure 5). In contrast to Theorem 1, this plane

does not have to be perpendicular to the $x^c y^c$–plane.

Theorem 2. *Given are a cone* $\underline{\mathbf{C}}(\hat{\underline{z}}_{k,j})$ *and a hyperboloid* $\mathbf{H}(\underline{p}^e_{k,j-1})$. *Furthermore, let*

$$d := \sqrt{(\hat{x}^m_{k,j} - x^e_{k,j-1})^2 + (\hat{y}^m_{k,j} - y^e_{k,j-1})^2}$$

denote the distance between the vectors $\left[\hat{x}^m_{k,j}, \hat{y}^m_{k,j}\right]^T$ *and* $\left[x^e_{k,j-1}, y^e_{k,j-1}\right]^T$. *If the following condition*

$$d > z^e_{k,j-1} + a^e_{k,j-1} \tag{13}$$

holds, then the hyperboloid $\mathbf{H}(\underline{p}^e_{k,j})$ *with*

$$\begin{bmatrix} x^e_{k,j} \\ y^e_{k,j} \end{bmatrix} = \begin{bmatrix} \hat{x}^m_{k,j} \\ \hat{y}^m_{k,j} \end{bmatrix} + \tfrac{1}{d}(m r_{apex} + c)\left(\begin{bmatrix} x^e_{k,j-1} \\ y^e_{k,j-1} \end{bmatrix} - \begin{bmatrix} \hat{x}^m_{k,j} \\ \hat{y}^m_{k,j} \end{bmatrix}\right) \tag{14}$$

$$z^e_{k,j} = m^2 r_{apex} + mc \tag{15}$$

$$a^e_{k,j} = r_{apex} - z^e_{k,j} \tag{16}$$

in which $m = \frac{z^e_{k,j}}{d}$, $c = d + \frac{(a^e_{k,j-1})^2 - (z^e_{k,j-1})^2}{2d}$ *and*

$$r_{apex} = \begin{cases} -\frac{c}{m-1} & \text{if } m^2 - 1 \neq 0 \\ -\frac{c}{2m} & \text{if } m^2 - 1 = 0 \end{cases}$$

has the following properties:

1. *The apex of* $\underline{\mathbf{C}}(\hat{\underline{z}}_{k,j}) \cap \mathbf{H}(\underline{p}^e_{k,j-1})$ *is* $\left[x^e_{k,j}, y^e_{k,j}, r_{apex}\right]^T$, *whereas* $r_{apex} = a^e_{k,j} + z^e_{k,j}$.

2. $\partial\underline{\mathbf{C}}(\hat{\underline{z}}_{k,j}) \cap \partial\mathbf{H}(\underline{p}^e_{k,j-1})$ *is a hyperbola that lies in a plane* E *with normal vector* $\left[x^e_{k,j-1} - \hat{x}^m_{k,j}, y^e_{k,j-1} - \hat{y}^m_{k,j}, z^e_{k,j}\right]^T$ *and position vector* $\left[x^e_{k,j}, y^e_{k,j}, r_{apex}\right]^T$.

3. $E \cap \partial\mathbf{H}(\underline{p}^e_{k,j}) = \partial\underline{\mathbf{C}}(\hat{\underline{z}}_{k,j}) \cap \partial\mathbf{H}(\underline{p}^e_{k,j-1})$

4. $\underline{\mathbf{C}}(\hat{\underline{z}}_{k,j}) \cap \mathbf{H}(\underline{p}^e_{k,j-1}) \subseteq \mathbf{H}(\underline{p}^e_{k,j})$

Proof. Can be shown with basic algebraic rules. $\square$

Remark 7. In analogy to Condition (5) in Theorem 1, Condition (13) states that the projection of the apex of $\underline{\mathbf{C}}(\hat{\underline{z}}_{k,j}) \cap \mathbf{H}(\underline{p}^e_{k,j-1})$ onto the $x^c y^c$–plane lies on the segment from $\left[\hat{x}^m_{k,j}, \hat{y}^m_{k,j}, 0\right]^T$ to $\left[x^e_{k,j-1}, y^e_{k,j-1}, 0\right]^T$.

Definition 4. The function $\mathcal{G}_2 : \mathbb{R}^7 \to \mathbb{R}^4$ is defined as

$$\mathcal{G}_2(\hat{\underline{z}}_{k,j}, \underline{p}^e_{k,j-1}) = \begin{cases} \mathcal{G}_2^*(\hat{\underline{z}}_{k,j}, \underline{p}^e_{k,j-1}) & \text{if (13) holds} \\ \begin{bmatrix} \hat{\underline{z}}_{k,j} \\ 0 \end{bmatrix} & \text{if } z^e_{k,j-1} + \\ & \quad a^e_{k,j-1} < 0 \\ \underline{p}^e_{k,j-1} & \text{otherwise} \end{cases}$$

in which $\mathcal{G}_2^* : \mathbb{R}^7 \to \mathbb{R}^4$ denotes the total function specified by Equations (14) - (16) that maps $\hat{\underline{z}}_{k,j}$ and $\underline{p}^e_{k,j-1}$ to $\underline{p}^e_{k,j}$.

6 Incorporating Knowledge about the Number of Measurements

In analogy to SSTE 1 in Section 4.2, SSTE 2 does not converge in general. Here, we cope with this behavior by incorporating further knowledge about the radius of the true
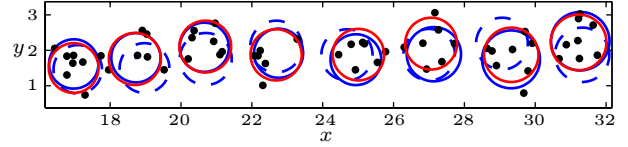
(a) State space: true (blue), estimated (red) and predicted (blue dashed) circular disc plotted over time. Black dots indicate measurements.
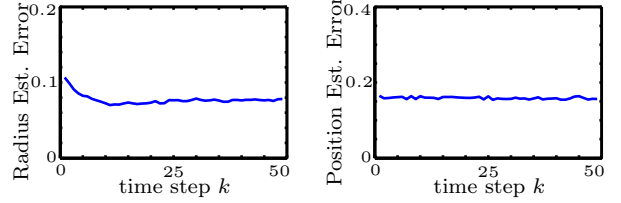
(b) Radius estimation error $|\mathrm{E}[r^e_k] - \tilde{r}_k|/\tilde{r}_k$ for 50 time steps averaged over 1000 simulation runs.

(c) Position estimation error $\|\mathrm{E}[[\boldsymbol{x}^e_k, \boldsymbol{y}^e_k]^T] - [\tilde{x}^c_k, \tilde{y}^c_k]^T\|_2$ for 50 time steps averaged over 1000 simulation runs.

Figure 6: Tracking an extended object: Simulation.

circular disc. A realistic assumption, which is often used in tracking algorithms for extended targets, is that the number of measurements received from the target object at a particular time step depends on its size. For instance, [2] suggests a Poisson distribution with an expectation proportional to the area of the extended target. Here, we assume that a conditional probability density $f(n_k|r_k)$, which specifies the number of measurements depending on the current radius of the extended object is available. In order to incorporate this knowledge into the estimation procedure SSTE 2, we maintain an addition random variable $\boldsymbol{r}^e_k$ that captures the knowledge about the true radius obtained from the number of measurements n_k. The accumulated knowledge at time step k is given by the random vector $\left[(\underline{\boldsymbol{p}}^e_k)^T, \boldsymbol{r}^e_k\right]^T$. $\left[(\underline{\boldsymbol{p}}^e_{k-1})^T, \boldsymbol{r}^e_{k-1}\right]^T$ can be propagated through the extended motion model according to

$$\begin{bmatrix} \boldsymbol{p}^p_k \\ \boldsymbol{r}^p_k \end{bmatrix} = \begin{bmatrix} \mathbf{A}_k & 0 & 0 \\ 0 & 1 & 0 \\ 0 & 0 & 1 \end{bmatrix} \begin{bmatrix} \boldsymbol{p}^e_{k-1} \\ \boldsymbol{r}^e_{k-1} \end{bmatrix} + \begin{bmatrix} \mathbf{B}_k \\ 0 \\ b^{(3)}_k \end{bmatrix} (\hat{u}_{k-1} + \underline{\boldsymbol{v}}_{k-1})$$

in which $b^{(3)}_k$ denotes the third row of $\mathbf{B}_k$. Again, we assume that $\left[(\boldsymbol{p}^e_{k-1})^T, \boldsymbol{r}^e_{k-1}\right]^T$ is Gaussian distributed such that $\left[\boldsymbol{p}^p_k, \boldsymbol{r}^p_k\right]^T$ is also Gaussian distributed and can be computed with the Kalman filter prediction step.

The prediction $\left[(\underline{\boldsymbol{p}}^p_k)^T, \boldsymbol{r}^p_k\right]^T$ can be updated with $\{\hat{\underline{z}}_{k,j}\}^{n_k}_{j=1}$ to obtain the posteriori pdf of $\left[(\underline{\boldsymbol{p}}^e_k)^T, \boldsymbol{r}^e_k\right]^T$ (given n_k) in the following way:

1. With $\underline{\boldsymbol{p}}^e_{k,0} := \underline{\boldsymbol{p}}^p_k$ and $\underline{\boldsymbol{p}}^e_{k,j} = \mathcal{G}_2(\underline{\boldsymbol{z}}_{k,j}, \underline{\boldsymbol{p}}^e_{k,j-1})$, the joint pdf of $\left[(\underline{\boldsymbol{p}}^e_k)^T, \boldsymbol{r}^e_k\right]^T := \left[(\underline{\boldsymbol{p}}^e_{k,n_k})^T, \boldsymbol{r}^e_k\right]^T$ can be computed (see SSTE 2).

2. Compute the posterior pdf $f(\underline{\boldsymbol{p}}^e_k, r^e_k \mid n_k)$ with Bayes'

rule

$$f(\underline{p}_k^e, r_k^e \mid n_k) = c \cdot f(n_k \mid r_k) \cdot f(\underline{p}_k^e, r_k^e) \;\; ,$$

where c is a normalization constant.

3. Compute the posterior pdf

$$f(\underline{p}_k^e, r_k^e \mid n_k, \{\boldsymbol{a}_k^e + \boldsymbol{z}_k^e \le \boldsymbol{r}_k^e\})$$

what corresponds to truncating infeasible values. This constraint arises from the fact that if $\boldsymbol{a}_k^e + \boldsymbol{z}_k^e > \boldsymbol{r}_k^e$, there is no disc with radius $\boldsymbol{r}_k^e$ in $\underline{\mathbf{H}}(\underline{p}_k^e)$. The (truncated) pdf can easily be approximated with a Gaussian distribution, in case $f(\underline{p}_k^e, r_k^e \mid n_k)$ is Gaussian (formulas for pdf truncation are given in [11]).

A proper point estimate for the radius is given by $\mathrm{E}[r_k^e]$ and a point estimate for the center is given by $\mathrm{E}\big[[\boldsymbol{x}_k^e, \boldsymbol{y}_k^e]^T\big]$ and covariance matrix $\mathrm{Cov}\big[[\boldsymbol{x}_k^e, \boldsymbol{y}_k^e, \boldsymbol{r}_k^e]^T\big]$. Note that if $\boldsymbol{r}_k^e$ is deterministic, the special case of known radius is obtained (see Remark 6).

7 Simulation

Figure 6 shows the result of a simulation run in which the true extended object is in fact a circular disc. At each time step, the measurement source $\underline{\tilde{z}}_{k,j}$ is sampled uniformly from the true circular disc and the measurement noise $\underline{w}_{k,j}$ is Gaussian with zero mean and covariance matrix $\mathrm{diag}\big([0.04, 0.04]^T\big)$. Note that SSTE 2 does not exploit any knowledge about the distribution of $\underline{\tilde{z}}_{k,j}$, which is assumed to be unknown. The number of measurements n_k produced by the true circular disc with radius r is approximately Gaussian distributed, i.e., $\boldsymbol{n}_k \sim \mathcal{N}^*(n_k; 5r, 0.4)$, where $\mathcal{N}^*$ denotes the Gaussian distribution with truncated negative values. Furthermore, a Gaussian prior pdf of $\boldsymbol{r}_1^e$ with mean 2 and variance 0.06 is given. The extended motion model is given by (9) with $\mathbf{A}_k = \mathbf{B}_k = \mathrm{diag}\big([1,1,1]^T\big)$, $\hat{\underline{u}}_{k-1} = [2,0,0]^T$ and $\mathbf{C}_k^v = \mathrm{diag}\big([0.02, 0.06, 0.001]^T\big)$. Figure 6a depicts a snippet of the state-space including the true disc (blue) for several time steps. The point estimates at each time step are plotted as red circles. Dashed circles represent the predicted circular disc. The estimated circular disc does not necessarily include all measurements, since the measurements are noise corrupted. In general, the higher the measurement noise, the more measurements lie outside the estimated disc. Figure 6b depicts the estimation error of the radius in percent $|\mathrm{E}[r_k^e] - \tilde{r}_k|/\tilde{r}_k$ for the first 50 time steps averaged over 1000 simulation runs. The overall average radius estimation error is 7.71%. Figure 6c shows the estimation error $\|\mathrm{E}[[\boldsymbol{x}_k^e, \boldsymbol{y}_k^e]^T] - [\tilde{x}_k^c, \tilde{y}_k^c]^T\|_2$ for the center for the first 50 time steps averaged over 1000 runs.

8 Conclusions and Future Work

In this paper, a novel method for tracking extended objects based on noisy position measurements was presented. In contrast to existing approaches, no assumptions about the distribution of the measurement sources on the extended object have been made. Therefore, a novel combined set-theoretic and stochastic estimator that uses random hyper-

boloids to express the uncertainty about the location and extent of the target object was derived. Future work will be concerned with extending the proposed method to higher dimensions and other geometric shapes like ellipsoids and rectangles.

References

[1] M. J. Waxman and O. E. Drummond, "A Bibliography of Cluster (Group) Tracking," *Signal and Data Processing of Small Targets 2004*, vol. 5428, no. 1, pp. 551–560, 2004.

[2] J. W. Koch, "Bayesian Approach to Extended Object and Cluster Tracking using Random Matrices," *Aerospace and Electronic Systems, IEEE Transactions on*, vol. 44, no. 3, pp. 1042–1059, July 2008.

[3] D. Salmond and N. Gordon, "Group and Extended Object Tracking," *IEEE Colloquium on Target Tracking: Algorithms and Applications*, pp. 16/1–16/4, 1999.

[4] K. Gilholm and D. Salmond, "Spatial Distribution Model for Tracking Extended objects," *Radar, Sonar and Navigation, IEE Proceedings*, vol. 152, no. 5, pp. 364–371, October 2005.

[5] P. Combettes and M. Civanlar, "The Foundations of Set Theoretic Estimation," *Acoustics, Speech, and Signal Processing, 1991. ICASSP-91., 1991 International Conference on*, pp. 2921–2924 vol.4, April 1991.

[6] U. D. Hanebeck, J. Horn, and G. Schmidt, "On Combining Statistical and Set Theoretic Estimation," *Automatica*, vol. 35, no. 6, pp. 1101–1109, June 1999.

[7] U. D. Hanebeck and J. Horn, "New Estimators for Mixed Stochastic and Set Theoretic Uncertainty Models: The General Case," in *Proceedings of the 2001 European Control Conference (ECC 2001)*, Porto, Portugal, September 2001.

[8] D. W. Hearn and J. Vijay, "Efficient Algorithms for the (Weighted) Minimum Circle Problem," *Operations Research*, vol. 30, no. 4, pp. 777–795, 1982.

[9] M. F. Huber and U. D. Hanebeck, "Gaussian Filter based on Deterministic Sampling for High Quality Nonlinear Estimation," in *Proceedings of the 17th IFAC World Congress (IFAC 2008)*, Seoul, Korea, July 2008.

[10] S. J. Julier and J. K. Uhlmann, "Unscented Filtering and Nonlinear Estimation," in *Proceedings of the IEEE*, vol. 92, no. 3, 2004, pp. 401–422.

[11] D. Simon, *Optimal State Estimation: Kalman, H Infinity, and Nonlinear Approaches*, 1st ed. Wiley & Sons, August 2006.